Mass Enhancement in the Superconducting State of Bi2Sr2CaCuO8+d : New Insights from Photoemission at (π-0)

A.V. Fedorov
A.D. Gromko
Y.-D. Chuang
J.D. Koralek
D.S. Dessau
Y. Aiura
Y. Yamaguchi
K. Oka
Yoichi Ando

University of Colorado
Advanced Light Source
Nat. Inst. of Adv. Indus. Sc. & Tech., JAPAN
Central Res. Inst. of Elec. Power Ind., JAPAN

Please, stay for the next talk of this session

$$ NSF Career-DMR-9985492; DOE DE-FG0300ER45809; ALS & SSRL are operated by the DOE, Office of Basic Energy Sciences

Our goal is to see it in superconductors

Outline

Detecting coupling of electrons to the collective modes with ARPES

History of the problem in HTSC

New data on BISCO samples at (π-0) and (π- π)

Coupling of electrons to collective modes

/phonons in a conventional superconductor 2H-$NbSe_2$,T_c ~7K/

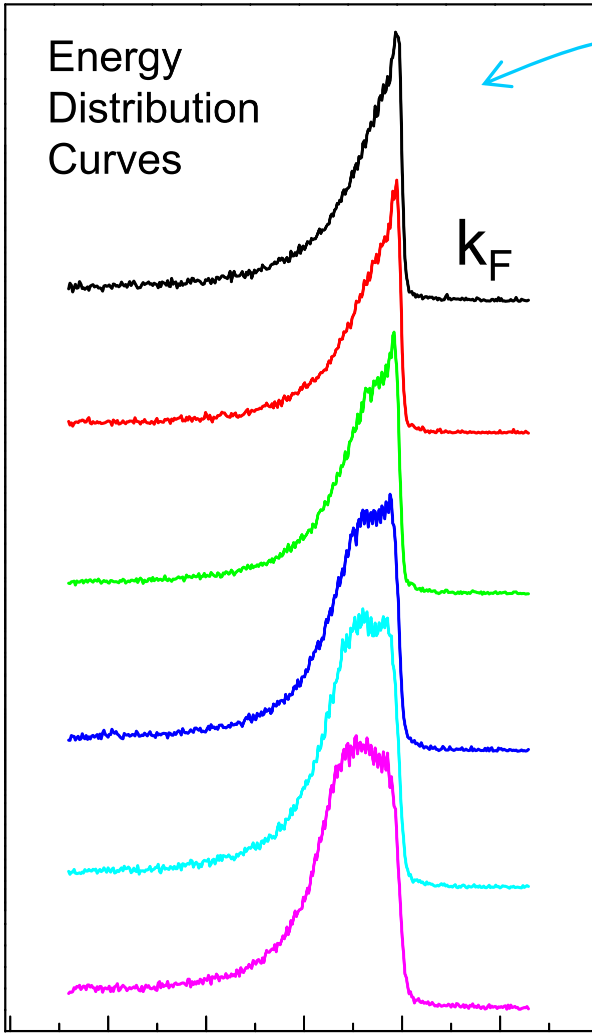

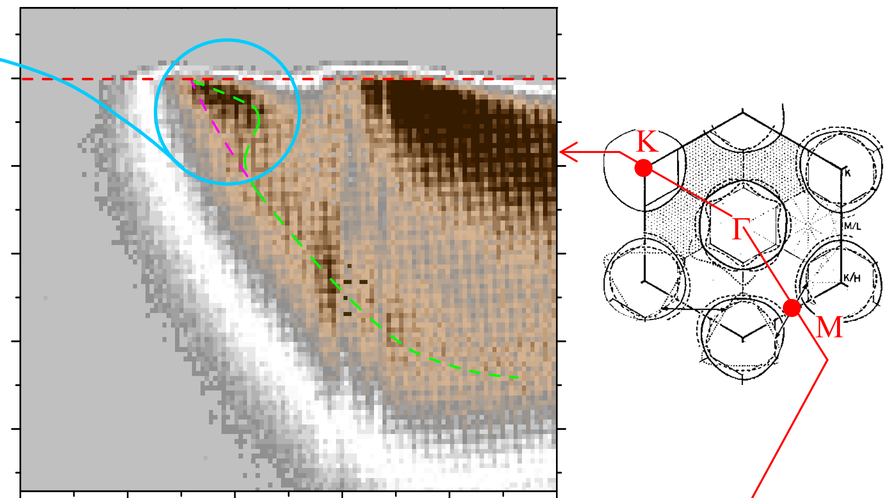

Coupling shows up as a "kink" in the dispersion and "peak-dip-hump" structure in EDC

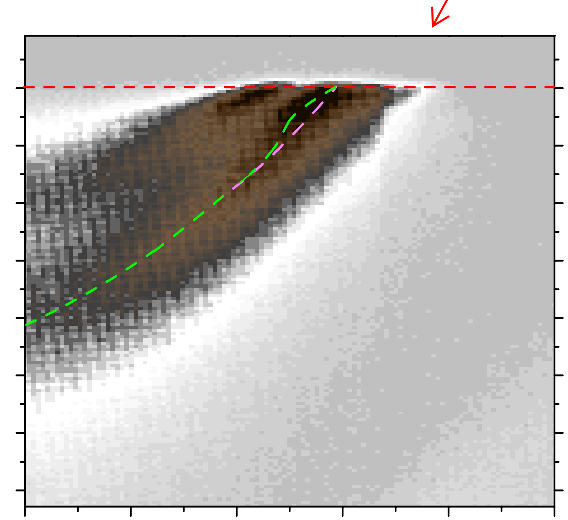

★ Note a well resolved bi-layer splitting

History

peak-dip-hump structure at (π-0) is due to the coupling to the "neutron resonance"

Z.-X. Shen & J.R. Schrieffer
PRL 78, 1771 (1997)

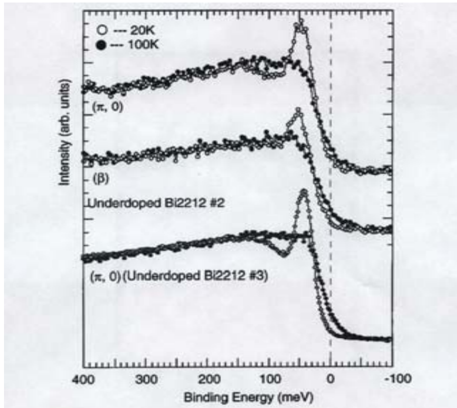

FIG. 2. ARPES data from normal and superconducting states of underdoped Bi2212 near $(\pi, 0)$. As illustrated in the inset of Fig. 1(β) is the Fermi surface crossing point along the $(\pi, 0)$ to (π, π) line and it is very close to $(\pi, 0)$. The upper two sets of curves were recorded with 35 meV energy resolution while the low set of curves was recorded with 20 meV energy resolution.

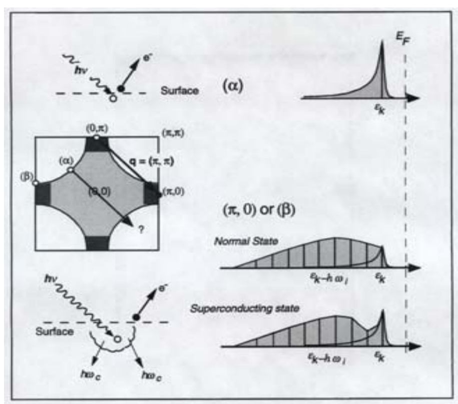

FIG. 3. Illustration of photoemission process and spectral shape in systems with weak (α) and strong couplings [(β) and $(\pi, 0)$]. The Fermi surface picture depicts the phase space considerations for the coupling between the quasiparticle and collective excitations near (π, π). The light shaded area indicates the filled states, and the dark shaded area indicates the flat band region near the Fermi level.

M.R. Norman & H. Ding
PRB 57, R11089 (1998)

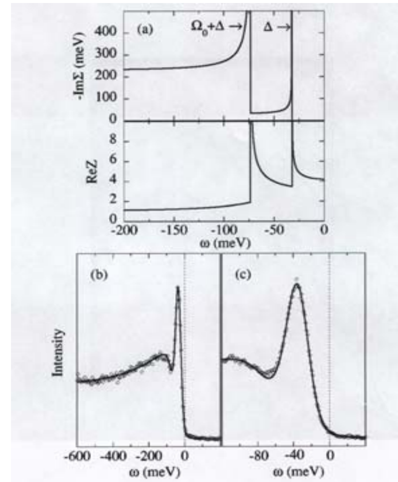

FIG. 3. (a) ImΣ and ReZ at $(\pi,0)$ from Eqs. (2) and (3) ($\Gamma_1=200$ meV, $\Gamma_0=30$ meV, $\Delta=32$ meV, $\Omega_0=1.3\Delta$). Comparison of the data at $(\pi,0)$ for (b) wide and (c) narrow energy scans with calculations based on Eqs. (1)–(3), with an added step edge background contribution.

J.C. Campuzano et al.
PRL 83, 3709 (1999)

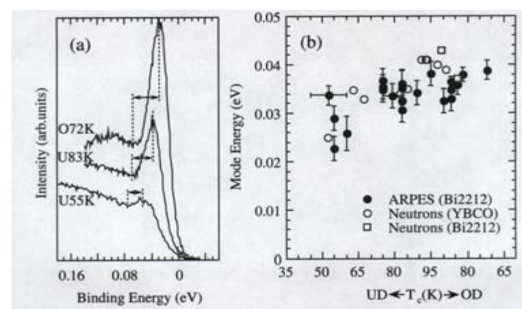

FIG. 5. Doping dependence of the mode energy: (a) Spectra at $(\pi, 0)$ showing the decrease in the energy separation of the peak and dip with underdoping. Peak and dip locations were obtained by independent polynomial fits and carefully checked for the effects of energy resolution. (b) Doping dependence of the collective mode energy inferred from ARPES together with that inferred from neutron data (for the latter, YBCO results as compiled in Ref. [5], Bi2212 results of Refs. [18] and [19]).

History

/nodal direction/

P.V. Bogdanov et al.,
PRL 85, 2581 (2000)

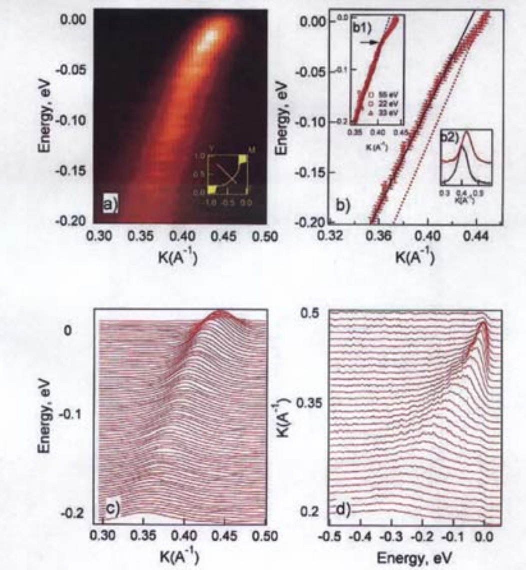

FIG. 1 (color). Panel (a) shows raw data obtained using Scienta angle mode for slightly overdoped ($T_c = 91$ K) $Bi_2Sr_2CaCu_2O_8$ along nodal direction (Γ-Y) of the BZ at 33 eV photon energy. The position of the cut is given in the inset. Panel (b) shows the dispersion of the quasiparticle determined from the MDC fits of the data in panel (a). The theoretical dispersion from LDA calculation is also included (dotted straight line). Energy is given relative to the Fermi energy. Inset (b1) shows the dispersion along this direction obtained at 22, 33, and 55 eV. Inset (b2) shows MDC's at 16 (blue) and 55 (red) meV BE. Dashed lines represent Lorenzian fits. Panels (c) and (d) show raw MDCs and EDCs, respectively.

Dispersion kink along (0,0)-(π,π) is due to the "neutron resonance" or phonons…

A. Kaminski et al.,
PRL 86, 1070 (2001)

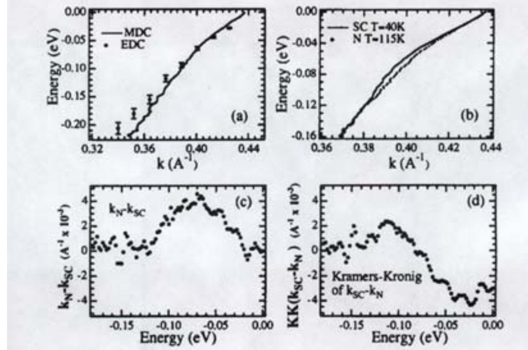

FIG. 2. ARPES data along the (π, π) direction at $h\nu = 28$ eV. (a) EDC dispersion in the normal state compared to the MDC dispersion. The EDCs are shown in Fig. 3d. (b) MDC dispersions in the superconducting state ($T = 40$ K) and normal state ($T = 115$ K). (c) Change in MDC dispersion from (b). (d) Kramers-Krönig transform of (c).

P.D. Johnson et al., PRL 87, 177007 (2001)

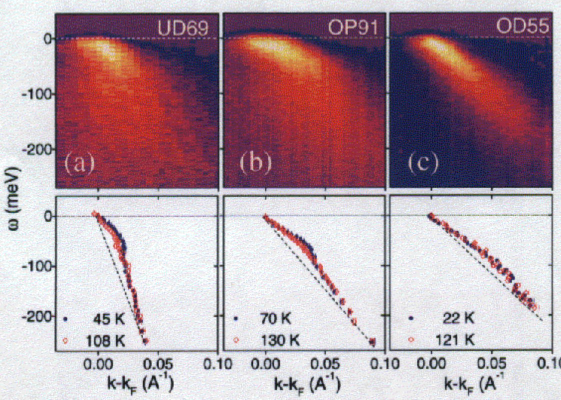

FIG. 1 (color). Upper panels: two dimensional photoemission intensities observed from (a) underdoped (UD), (b) optimally doped (OP), and (c) overdoped (OD) samples. The superconducting transition temperatures are indicated. Lower panels: the dotted lines indicate the MDC deduced dispersions for both the superconducting (blue dots) and normal states (open red diamonds) corresponding to the different samples in the panels above.

History
/theoretical work/

PDH structure at (π-0)

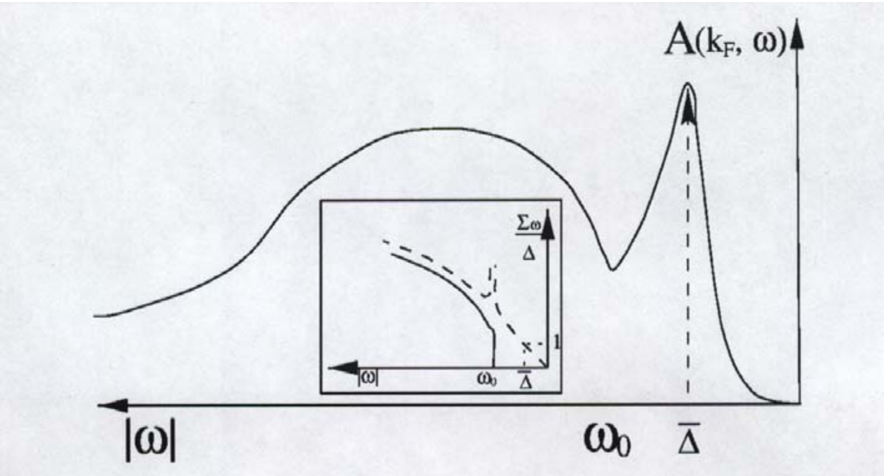

FIG. 2. Same as in Fig. 1 but at strong coupling. The resonance and onset frequencies are presented in the text. The spin resonance frequency $\Omega_{res} \propto \xi^{-1}$, is equal to the distance between the measured gap $\bar{\Delta}$ and the dip frequency ω_0. The hump frequency differs from $\bar{\Delta}$ roughly by $\xi^{0.7}$.

Ar. Abanov & A. V. Chubukov
PRL 83, 1652 (1999)

Kink along the node

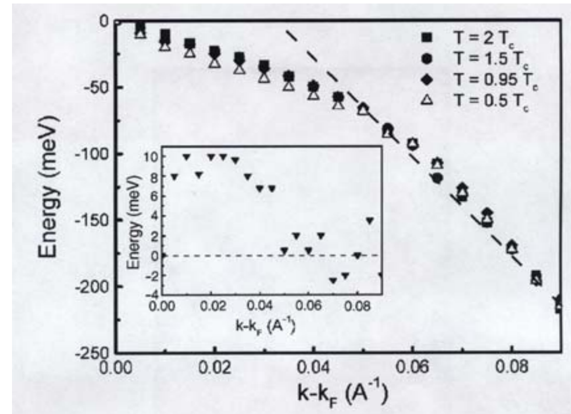

FIG. 2. Positions of the peaks in the spectral density $A(\mathbf{k}, \omega)$ versus $\mathbf{k} - \mathbf{k}_F$ (energy dispersion) along the $(0,0) \rightarrow (\pi, 0)$ direction of the BZ calculated within the FLEX approximation. This has to be compared with the position of the peaks derived from the momentum distribution curve (MDC) for a hole-doped superconductor as measured in experiment. The curves show a "kink" at energies about $\hbar\omega \approx 65 \pm 15$ meV. The dashed line is a guide to the eyes. We find small changes due to superconductivity which almost coincide with the kink position. Inset: Change in the peak position in $A(\mathbf{k}, \omega)$ in the superconducting state ($T = 0.5 T_c$). The results are in fair agreement with ARPES data [3].

D. Manske, I. Eremin
And K.H. Bennemann
PRL 87, 177005 (2001)

Recent progress in ARPES and improvements in the sample quality enabled the direct observation of bonding and anti-bonding bands in BISCO

Hence, we had a good reason to go back and look at PDH and kinks, particularly at (π-0), where splitting is strongest

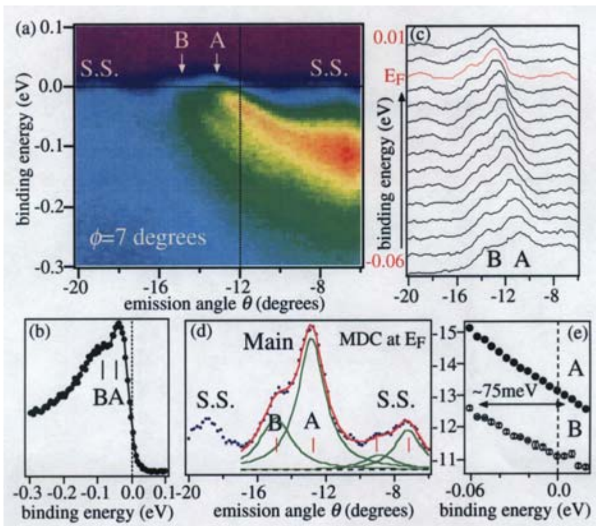

FIG. 2 (color). (a) False color plot of E vs emission angle θ for the $\phi = 7°$ cut [white line in Fig. 1(a)]. (b) EDC at $\theta = -12°$ from panel (a) (vertical black dashed line). Two distinct features, A and B, can be clearly seen in this EDC. (c) MDCs from panel (a) from binding energies +10 to −60 meV, with 5 meV steps. (d) The MDC at E_F (blue dots), including a deconvolution of the main band (red line shows the fitting result) into two Lorentzian functions A and B (green lines) plus two corresponding features in superstructure band (green lines) on top of a linear background (black dashed line). (e) The energy dependence of the θ value of MDC peaks A (closed circles) and B (open circles). The error bar from the fitting is smaller than the symbol size.

Y.-D. Chuang et al., PRL 87, 117002 (2001)

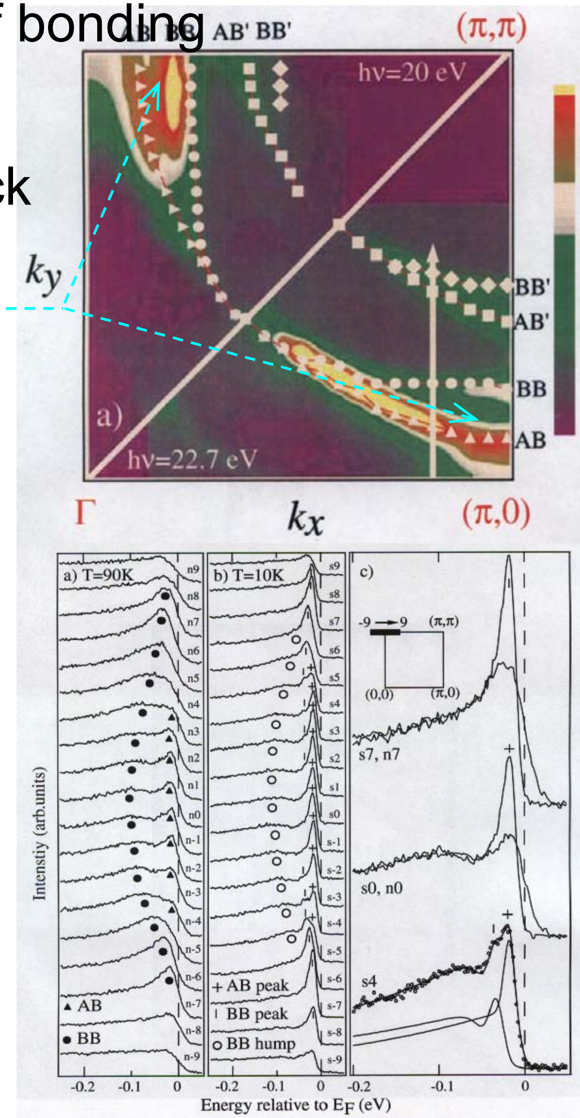

FIG. 3. ARPES spectra taken on OD65 with He-Iα light for (a) normal state, and (b) superconducting state. The angular resolution is 0.56°. (c) shows selected spectra from (a) and (b). Note that the fit of s4 is not unique. The spectra are taken along $(-0.24\pi, \pi)$ − $(0.24\pi, \pi)$, and labeled from −9 to 9 as shown in the inset of (c).

D.L. Feng et al., PRL 86, 5550 (2001)

New Data

Kink along the node in underdoped and overdoped samples

Kink /S-shaped / is well—resolved above and below T_C and it does`t change much at transition

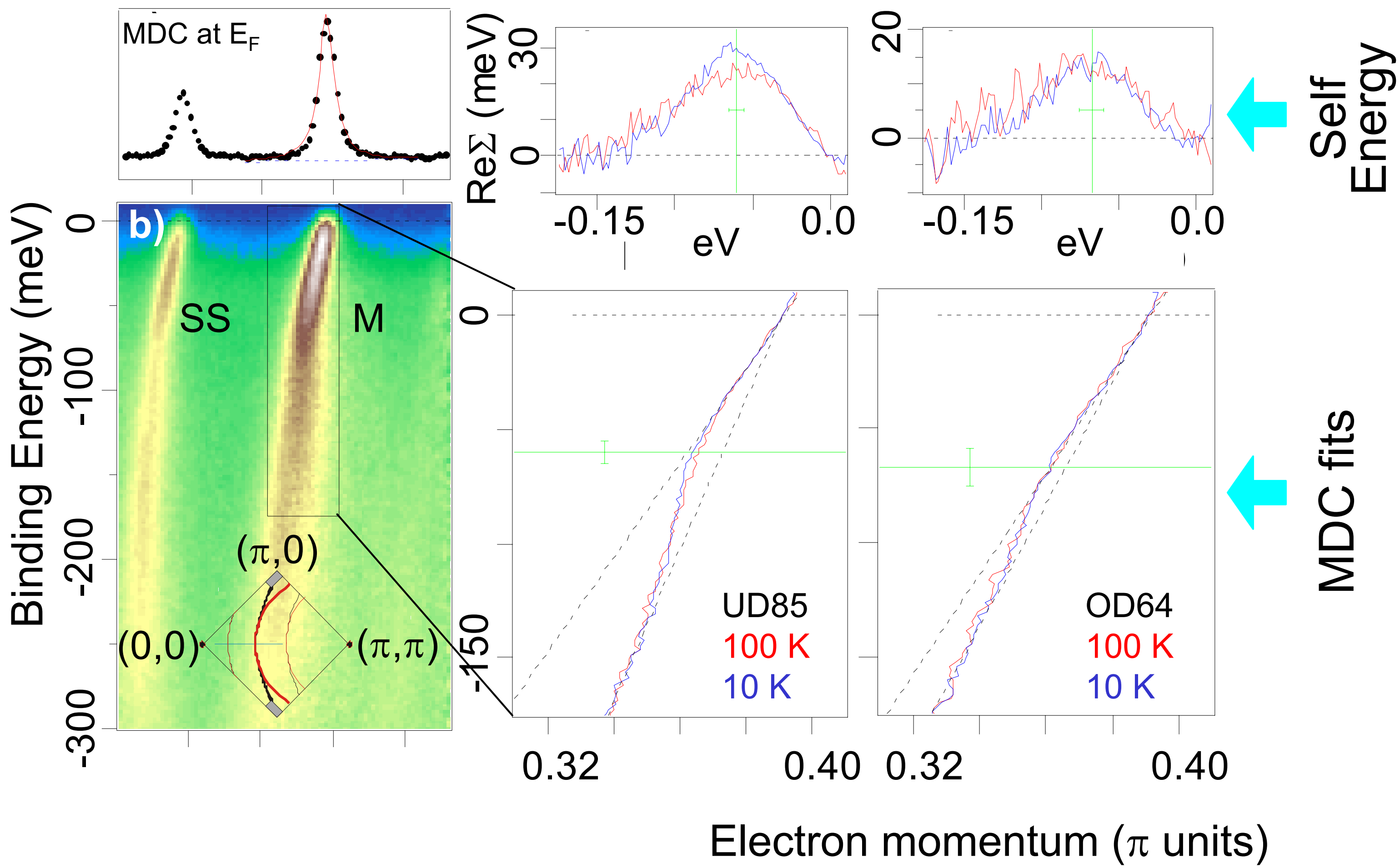

Kink at (π-0)

bi-layer splitting and superstructure are clearly resolved

No sign of a kink in a normal state

It shows up only below T_C

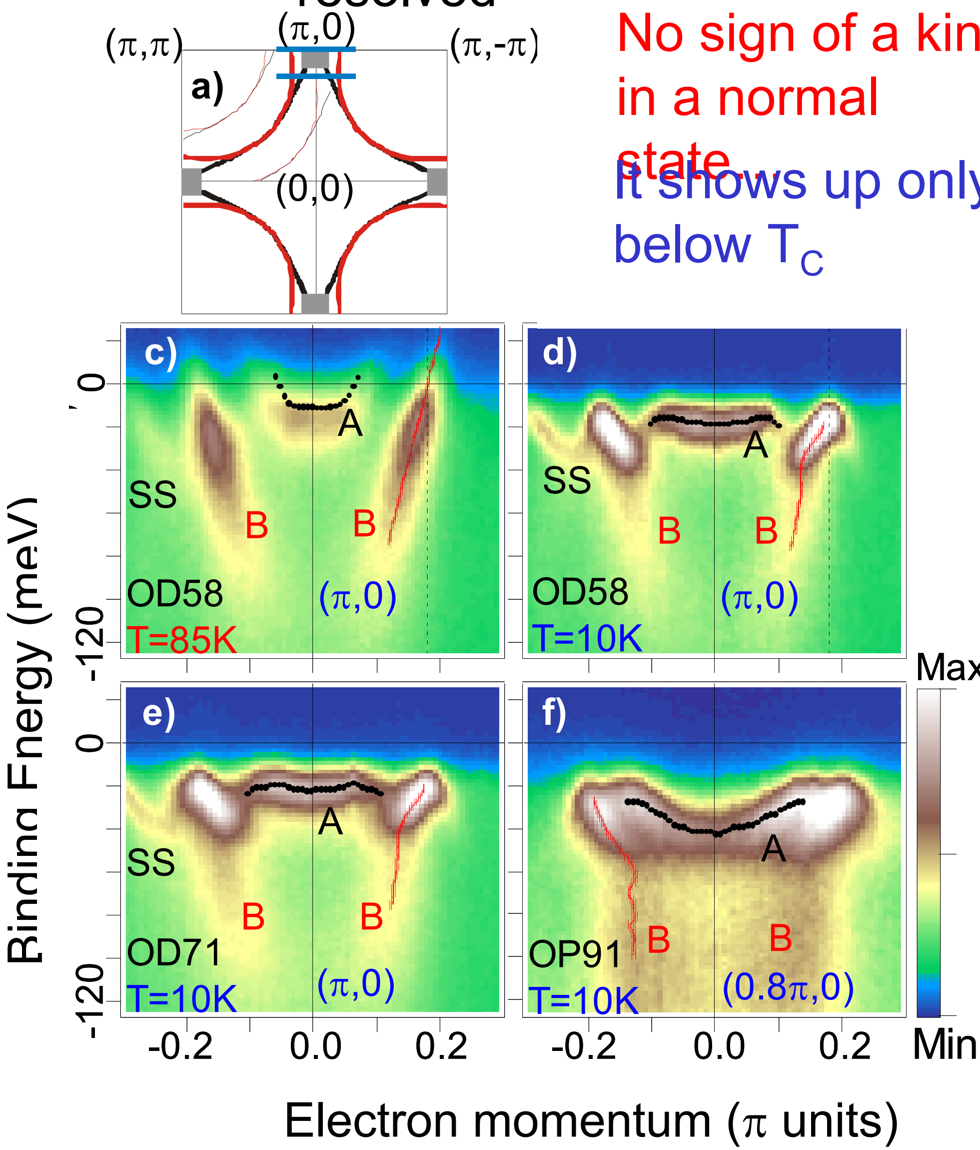

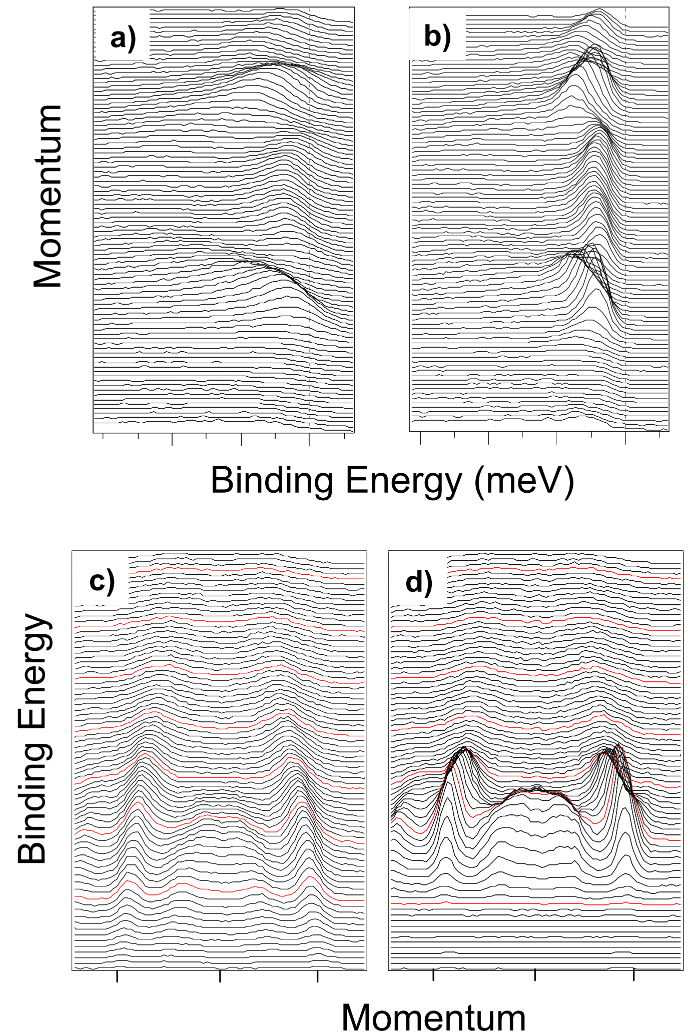

Overdoped sample, T_C= 71 K

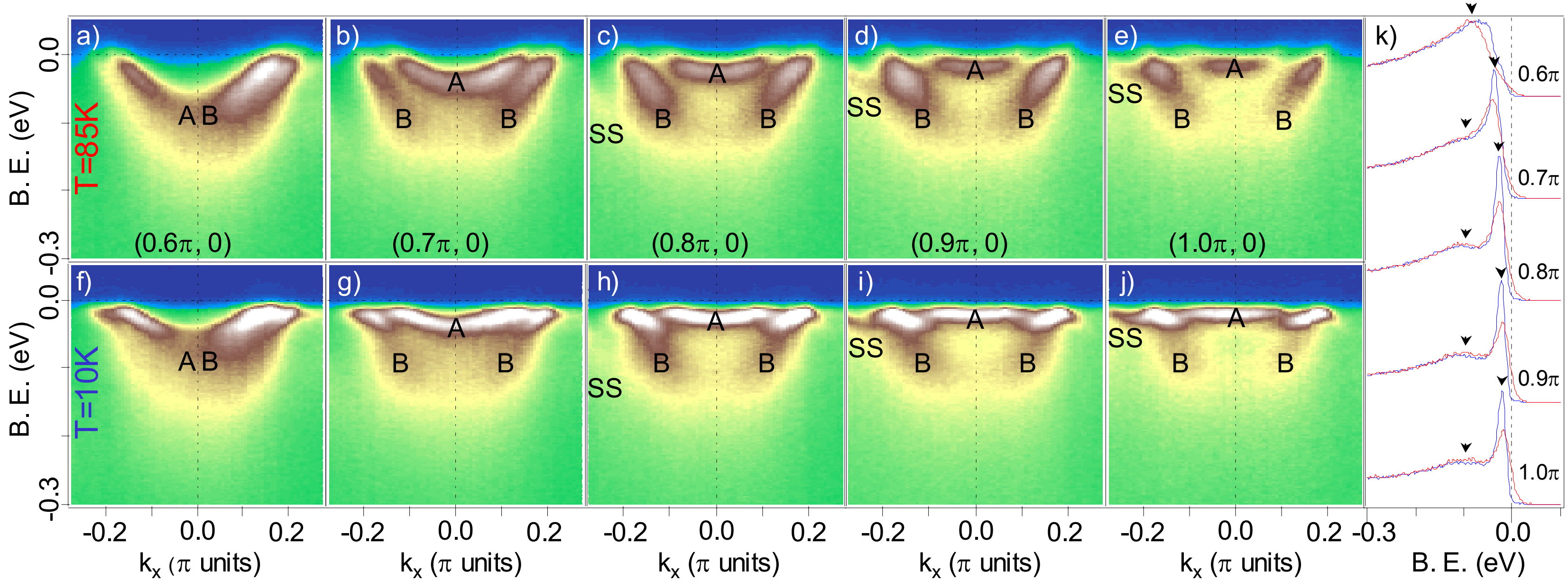

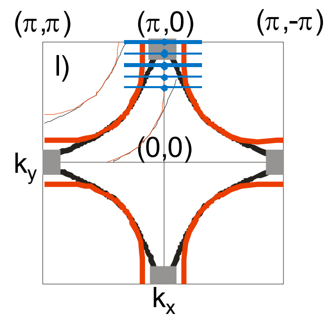

Normal and superconducting state data at different locations in the Brillouin zone

Optimally doped sample, T_C= 91 K

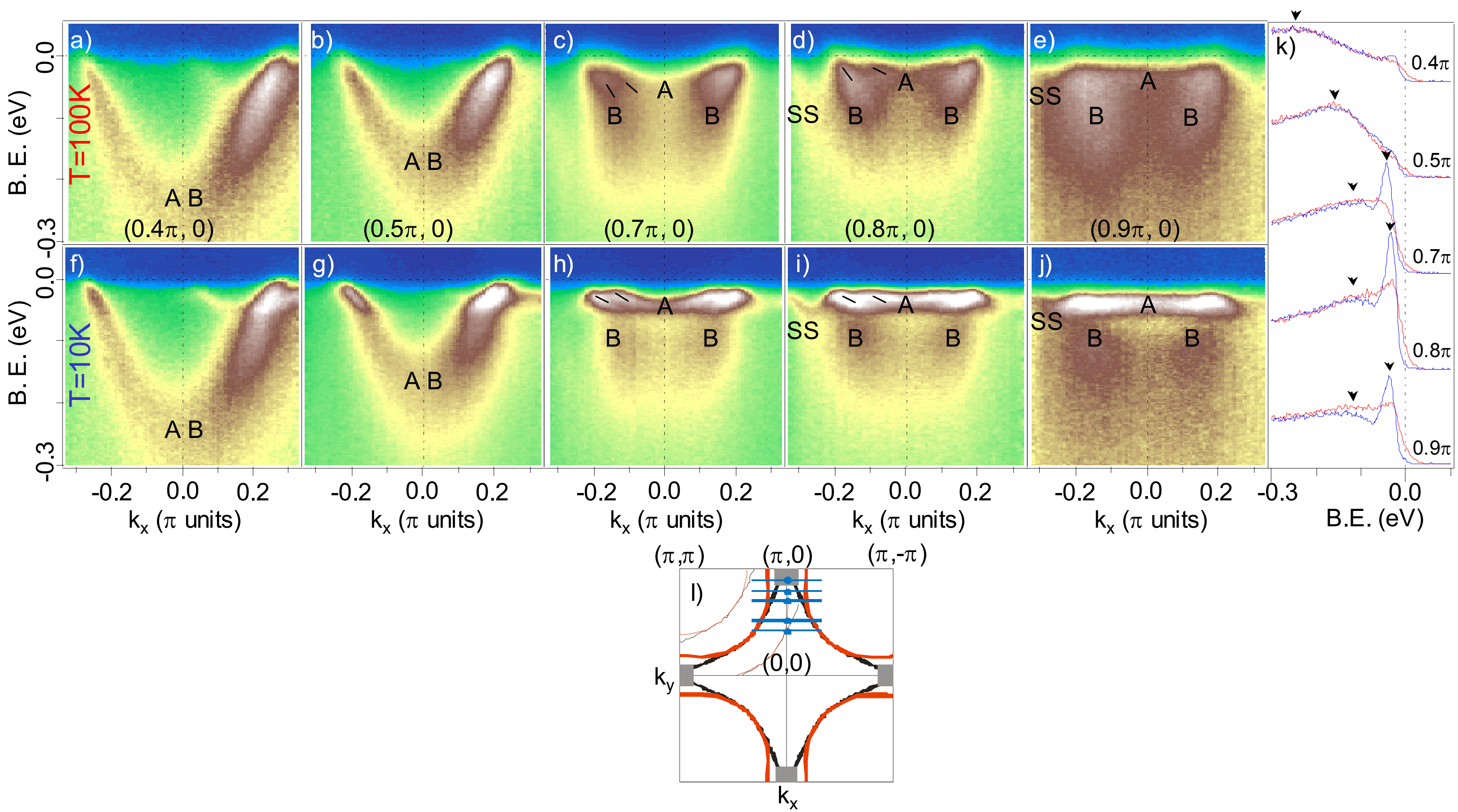

Deconvolving peak dip hump structure due to the strong coupling and bi-layer splitting

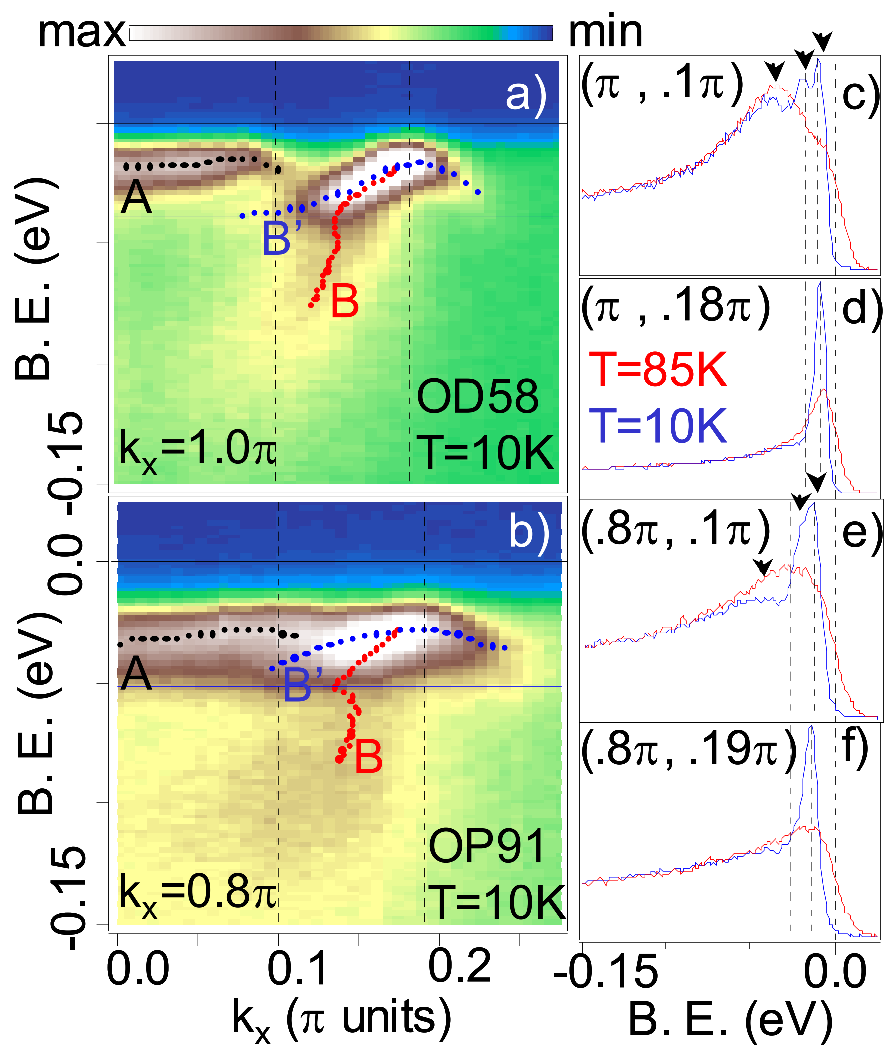

Conclusions

Deconvolving bonding and anti-bonding bands is essential for studying coupling effects close to (π-0)

Mass enhancement at (π-0) in the superconducting state of BISCO, along with resolving both bands has been observed for the first time

Data at (π,π) are consistent with the previous studies and show kink above and below the transition

Detailed analysis of the newly observed kink at (π-0) will be presented in the next talk